Journal of Thermal Engineering
Yildiz Technical University Press, Istanbul, Turkey
Vol. 2, Special Issue 4, No. 4, pp. 897-906, July, 2016.

http://eds.yildiz.edu.tr/journal-of-thermal-engineering/Articles
Manuscript Received December 20, 2015; Accepted February 02, 2016

This paper was recommended for publication in revised form by Associate Editor Tolga Taner

USING PHASE CHANGE MATERIALS IN PHOTOVOLTAIC SYSTEMS FOR CELL TEMPERATURE REDUCTION: A FINITE DIFFERENCE SIMULATION METHOD

***Panagiotis Kladisios**
Laboratory of Heat Transfer and Thermal Processes, School of Mechanical Engineering, National Technical University of Athens, Greece

Athina Stegou-Sagia
Laboratory of Heat Transfer and Thermal Processes, School of Mechanical Engineering, National Technical University of Athens, Greece

Keywords: photovoltaic, phase change materials, effective heat capacity, finite difference method
** Corresponding author: 00 210 7523206*
E-mail address: pkladisios@hotmail.gr

ABSTRACT

Photovoltaic manufacturers rate their modules based on their maximum power output. This nominal power corresponds to the commonly accepted standard test conditions (STC: cell temperature T_{cell}=25 ºC, insolation G=1 kW/m^2, air mass AM=1.5). In reality, insolation is lower and cell temperature higher, both being factors that affect power generation in a negative fashion. In the present paper, the possibility of cell temperature reduction will be investigated using one of the proposed methods of thermal control, phase change materials. The photovoltaic module, both as a unit and as a system in direct contact with a phase change material, will be simulated using a finite difference method.

INTRODUCTION

The combination of global climate change and the continuous increase of energy demand on a world scale has made the utilization of renewable energy sources of paramount significance. One of the most promising renewable energy technologies is the photovoltaic (PV). PV modules benefit from a practically endless fuel source, produce no emissions or waste of any kind and exhibit remarkable longevity due to the lack of moving parts (some manufacturers guarantee more than 30 years of functionality). Photovoltaic manufacturers rate their modules based on their maximum power output, power that corresponds to the commonly accepted standard test conditions (STC: cell temperature T_{cell}=25 ºC, insolation G=1 kW/m^2, air mass AM=1.5), conditions that rarely occur outside a controlled environment such as a laboratory [1]. In most cases insolation is lower and cell temperature higher, both being factors that affect power generation in a negative fashion. Solar cells can reach temperatures higher than that of air by 20-30 ºC [2].

One of the proposed methods for the reduction of solar cell temperature and, consequently, for the increase of generated power is the use of phase change materials (PCM). PCMs are renowned for their ability to absorb and release large amounts of heat under small temperature ranges, an attribute that makes them ideal mediums of thermal control [3-5].

The heat transfer within the PV-PCM system is described by a partial differential equation. There are several numerical techniques that deal with the numerical solution of such equations with the most dominant being the finite element method (FEM), the finite volume method (FVM) and the finite difference method (FDM).

Finite element method involves the discretization of a continuous domain into a set of discrete sub-domains, called finite elements, and the integration of the differential equation inside each finite element using an error minimization criterion. This method is difficult to implement but can handle complex geometries and boundaries with relative ease. It is commonly used in, but not limited to, problems of structural mechanics. Finite volume method involves the integration of the governing equations inside sub-volumes of the domain. Being conservative, it satisfies the conservation of mass, energy and momentum. This method is used mostly in computational fluid dynamics (CFD). Finite difference method deals with the approximation of the derivatives of the differential equations with finite differences using Taylor expansions. FDM offers speed and ease of implementation and it is popular for problems with simple geometries [6].

In the present paper the heat transfer in the PV-PCM system will be simulated using a finite difference method (FDM) approach. Out of the proposed FDM schemes, the most popular are the explicit, the implicit and the Crank-Nicolson scheme. The explicit scheme is the least accurate and conditionally stable but, at the same time, the easiest to apply and the least numerically intensive. The implicit scheme is ideal for large time steps. Despite the fact that it is numerically intensive, demanding the solution of a linear system of equations, the unconditional numerical stability and convergence, the convenient tridiagonal form of the system and the capacity to use large time steps lead to a considerable decrease in computational time. The Crank-Nicolson scheme is the most accurate, but for very small time steps [6-8]. For the purposes of this paper the implicit scheme was chosen, since it was based on hourly meteorological data and a large time step was required.

The system is treated as a multi-layered plate, one layer of which is a phase change material that changes phase during the course of a day. The two of the most dominant methods for simulating the thermal behavior of a PCM are the enthalpy method and the effective heat capacity method [9]. The enthalpy method introduces the enthalpy into the governing equation. This model guarantees the isothermal nature of the phase change and fully defines the quantities of latent and sensible heat. It is difficult to implement, but it is appropriate when details (e.g. position of the solid-liquid interface) about the phase change are needed. The effective heat capacity method was used to simulate the thermal behavior of the phase change material. According to this method, the PCM's heat capacity is calculated as a function of temperature, a fact that simplifies the thermal study of the system [9-10].

It should be noted that the algorithm that calculates the temperature distribution of the PV-PCM system was written in Python (2.7), a modern programming language that accommodates a plethora of tools and above all simple syntax. The main reasons for which Python was preferred are the advanced array and plot libraries (numpy and matplotlib respectively) [8].

MATHEMATICAL MODELING

The photovoltaic unit that was chosen for modeling is Kyocera's KC175GHT-2, a high efficiency (over 16 %) polycrystalline module [11]. The process of making polycrystalline silicon (p-Si) is much easier and, therefore, costs less in comparison with other commercial types such as monocrystalline and thin-film panels [12].

Assuming a simplified geometry, the PV-PCM system consists of the following layers:

- tempered (soda-lime) glass
- PET (polyethylene terephthalate) plastic panel, upon which solar cells of negligible thickness are printed.
- plastic bag that contains the PCM (LDPE, low density polyethylene)
- layer of phase change material
- plastic bag that contains the PCM (LDPE, low density polyethylene)

A figure of the simplified geometry as well as a table of properties follow (figure 1 and table 1 respectively) [13]. The thermo-physical properties of the phase change materials will be described later.

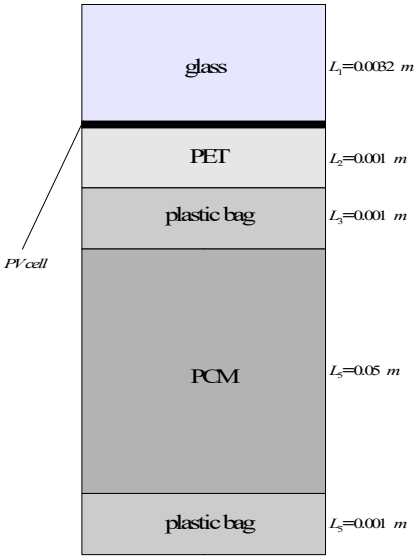

Figure 1 Simplified PV-PCM system geometry

Table 1 Material properties

Property	1:glass	2:PET	3:plastic bag	4:PCM	5:plastic bag
L[m]	0.0032	0.001	0.001	0.05	0.001
k [W/mk]	1.05	0.195	0.36	k_{pcm}	0.36
ρ [kg/m^3]	2440	1470	920	ρ_{pcm}	920
C_p[kJ/kgK]	0.72	1.075	2.3	$C_{p,pcm}$	2.3

HEAT DIFFUSION EQUATION

The general form of the heat diffusion equation is:

$$\frac{\partial}{\partial x}\left(k\frac{\partial T}{\partial x}\right)+\frac{\partial}{\partial y}\left(k\frac{\partial T}{\partial y}\right)+\frac{\partial}{\partial z}\left(k\frac{\partial T}{\partial z}\right)+\dot{\Phi}=\rho C_p\frac{\partial T}{\partial t} \quad (1)$$

The above equation is the result of the conservation of energy within a finite control volume. Its solution provides the temperature distribution T(x,y,z) as a function of time t. The first three terms $\frac{\partial}{\partial x}\left(k\frac{\partial T}{\partial x}\right)$, $\frac{\partial}{\partial y}\left(k\frac{\partial T}{\partial y}\right)$, $\frac{\partial}{\partial z}\left(k\frac{\partial T}{\partial z}\right)$ describe the net heat flux that is conducted into the control volume for the x, y, z direction respectively. $\dot{\Phi}$ is the rate that energy is being produced or consumed inside the control volume.

$\rho C_p \frac{\partial T}{\partial t}$ is the rate of change of energy content inside the control volume [14-16].

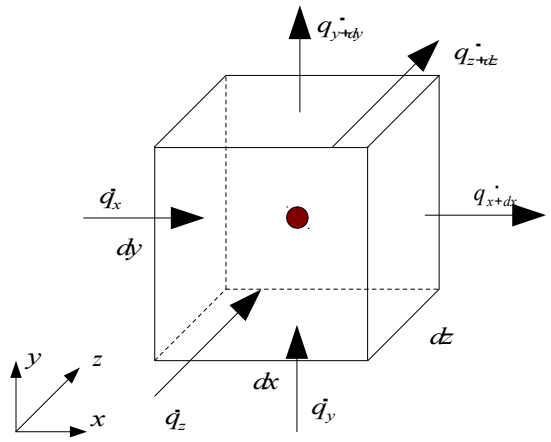

Figure 2 Finite control volume of dimensions dx, dy, dz [14]

It is quite common for simplified versions of the heat equation to be used. For one-dimensional heat transfer, constant thermal conductivity and no heat sources or sinks inside the control volume the equation assumes the following form:

$$\frac{\partial T}{\partial t} = a\frac{\partial^2 T}{\partial x^2} \tag{2}$$

where $a = \frac{k}{\rho C_p}$ [m/s^2] is the thermal diffusivity, a measure of the material's ability to conduct thermal energy relative to its ability to store it [15]. In cases of simple geometries such as a composite slab, where one dimension is much smaller than the rest, a good approximation of the internal heat transfer can be achieved using the one-dimensional heat equation. The temperature changes along the other two dimensions are considered to be insignificant in comparison to the lesser dimension [16]. The simplified geometry and the low thickness/surface ratio allow the use of an one-dimensional heat transfer approach to the problem at hand. Therefore, equation (2) was used to describe the heat transfer process in the PV-PCM system.

FINITE DIFFERENCE METHOD

As it was previously mentioned, the equation that describes the one-dimensional heat transfer within the PV-PCM system, is:

$$\frac{\partial T}{\partial t} = a\frac{\partial^2 T}{\partial x^2} \tag{2}$$

and will be solved with the finite difference method (FDM). The most popular expressions of this method are explicit, implicit and Crank-Nicolson, each with its own merits and shortcomings. For the purposes of this thesis an implicit approach will be used. The implicit scheme is always numerically stable and convergent but numerically intensive as it demands the solution of a linear system of equations. The convenient shape of the linear system, which is tridiagonal, and the fact that the scheme allows the use of large time steps dt lead to a considerable reduction of computational time compared to the other schemes [6-8].

Before the heat equation is transformed into a finite difference equation, a spatial discretization must take place. Since a multi-layered body is involved, a non-uniform grid will be used. A non-uniform mesh allows the use of variable spatial step throughout the system and, therefore, increased accuracy in areas where high temperature gradients take place (temperature changes rapidly). We assume finite volumes of length dx, different for each material. The nodes are positioned on the center of each volume and the number of nodes is also different for each material. About 5 nodes per mm of thickness were used (n_1=15, n_2=5, n_3=5, n_4=250, n_5=5). Nodes i_{12}, i_{23}, i_{34}, i_{45} and i_{54} represent nodes where layer change has already "taken place" with i_{12} being the cell node. The finite volumes are placed in such a way that the first (i=0) and the last node (i=n-1) coincide with the physical barriers of the PV-PCM system. In addition, two consecutive discretizations, which correspond to two separate materials, must “meet” on the common surface where layer change occurs. That would mean that no node is placed on a common surface. Otherwise, the thermo-physical properties of such a node would be impossible to define (having the properties of two materials at the same time). For instance, the solar cell node i_{12}, where layer changes from glass to PET, is placed on the side of the second material and for a mesh thick enough would be sufficiently close to their common surface. That also corresponds with the fact that solar cells are “printed” upon the PET panel. A schematic representation is depicted in figure 3.

According to the implicit expression, a forward difference will be used for the temporal derivative. Concerning the spatial derivative, a central difference of a non-uniform grid at the next point in time (p+1) will be used [6]. At this point, it should be clarified that p is the index of the point in time (p=0, 1, 2,...,m-2, m-1, where m is total number of points in time).
Time derivative:

$$\frac{\partial T}{\partial t} = \frac{T_i^{p+1} - T_i^p}{dt} \tag{3}$$

Space derivative:

$$\frac{\partial^2 T}{\partial x^2} = \frac{dx_i T_{i-1}^{p+1} - (dx_{i-1} + dx_i)T_i^{p+1} + dx_{i-1}T_{i+1}^{p+1}}{\frac{1}{2}dx_{i-1}dx_i(dx_{i-1} + dx_i)} \tag{4}$$

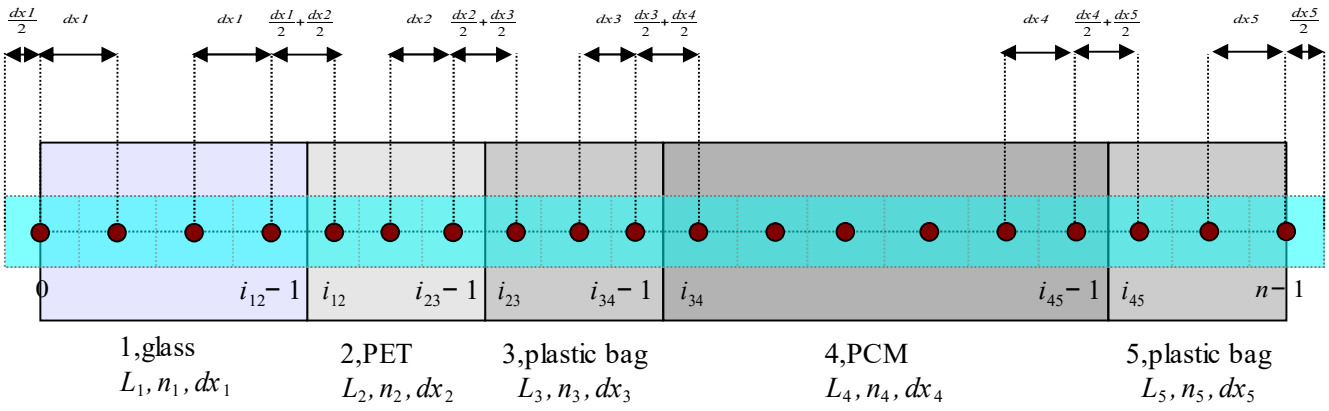

Figure 3 Schematic representation of the PV-PCM system's spatial discretization

Apparently for $dx_{i-1} = dx_i$, the above equation becomes the central difference for a uniform grid. Replacing (3) and (4) in (2):

$$\frac{T_i^{p+1} - T_i^p}{dt} = \frac{k_i}{\rho_i C_{p_i}} \frac{dx_i T_{i-1}^{p+1} - (dx_{i-1} + dx_i) T_i^{p+1} + dx_{i-1} T_{i+1}^{p+1}}{\frac{1}{2} dx_{i-1} dx_i (dx_{i-1} + dx_i)}$$

$$T_i^{p+1} - T_i^p = \frac{k_i dt}{\rho_i C_{p_i} dx_{i-1} dx_i (dx_{i-1} + dx_i)} \times$$
$$\times (dx_i T_{i-1}^{p+1} - (dx_{i-1} + dx_i) T_i^{p+1} + dx_{i-1} T_{i+1}^{p+1})$$

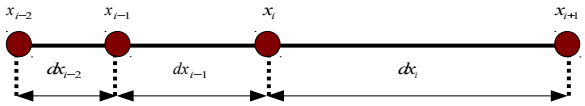

Figure 4 One-dimensional non-uniform grid

For simplicity we assign a coefficient r_i to each node i:

$$r_i = \frac{k_i dt}{\rho_i C_{p_i} dx_{i-1} dx_i (dx_{i-1} + dx_i)}$$

$$T_i^{p+1} - T_i^p = r_i (dx_i T_{i-1}^{p+1} - (dx_{i-1} + dx_i) T_i^{p+1} + dx_{i-1} T_{i+1}^{p+1}) \rightarrow$$

$$T_i^{p+1} - T_i^p = r_i dx_i T_{i-1}^{p+1} - r_i (dx_{i-1} + dx_i) T_i^{p+1} + r_i dx_{i-1} T_{i+1}^{p+1} \rightarrow$$

$$T_i^{p+1} - r_i dx_i T_{i-1}^{p+1} + r_i (dx_{i-1} + dx_i) T_i^{p+1} - r_i dx_{i-1} T_{i+1}^{p+1} = T_i^p \rightarrow$$

$$(-r_i dx_i) T_{i-1}^{p+1} + (1 + r_i (dx_{i-1} + dx_i)) T_i^{p+1} - (r_i dx_{i-1}) T_{i+1}^{p+1} = T_i^p \quad (5)$$

Equation (2) is transformed to the above and is valid only for the internal nodes (i=1,2,…,n-2.). For the external nodes i=0 and i=(n-1) boundary conditions must be applied. It should be noted that hourly time steps (dt=3600s) will be used.

BOUNDARY CONDITIONS

A figure of the energy exchange between the PV-PCM system and its environment follows.

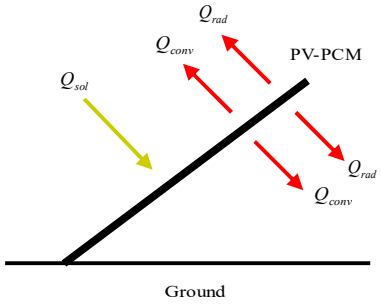

Figure 5 Energy exchange between PV-PCM system and its environment

Both surfaces lose heat due to convection and radiation and at the same time the upper surface (exposed to the sun) gains heat due to solar radiation.

Upper surface (i=0)

As it was previously mentioned, the upper surface presents heat gain due to solar radiation Q_{sol} and heat losses due to radiation Q_{rad} and convection Q_{conv}.

$$Q_{cond}^{p+1} = Q_{sol}^{p+1} - Q_{conv}^{p+1} - Q_{rad}^{p+1} \quad (6)$$

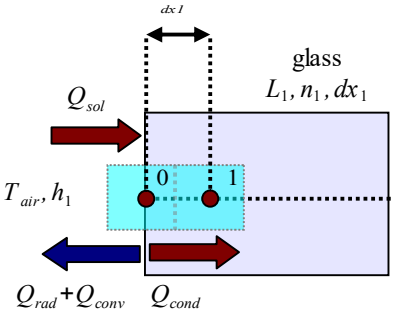

Figure 6 Upper surface boundary condition (i=0)

-Thermal gain due to insolation [17]:

$$Q_{sol}^{p+1} = a_{glass} G_T^{p+1} \quad (7)$$

where α_{glass}=0.96 [-] [13], is the absorptivity of glass and G_T [kW/m^2] is the total solar radiation of an inclined surface (in our case the upper surface of the PV-PCM system).

-Thermal losses due to radiation [15-16]:

$$Q_{rad}{}^{p+1} = \varepsilon\sigma(T_0{}^{p+1^4} - T_{air}{}^{p+1^4}) \quad (8)$$

The introduction of an unknown temperature to the fourth power would transform the linear system into a non-linear, thus perplexing the computational process. In order to simplify our calculations, for relatively small temperature differences we can assume a radiation heat transfer coefficient h_{r1}, such as [16,19]:

$$Q_{rad}^{p+1} = h_{r1}(T_0^{p+1} - T_{air}^{p+1}) \quad (9)$$

-Thermal losses due to free convection:

$$Q_{conv}^{p+1} = h_{c1}(T_0^{p+1} - T_{air}^{p+1}) \quad (10)$$

where h_{c1} is the convection coefficient.
We can assume a combined heat transfer coefficient that takes convection and radiation into consideration [19-20]:

$$h_1 = h_{c1} + h_{r1} \quad (11)$$

$$Q_{conv}^{p+1} + Q_{rad}^{p+1} = h_1(T_0^{p+1} - T_{air}^{p+1})$$

Considering the above, (6) becomes:

$$-k_1 \frac{T_1^{p+1} - T_0^{p+1}}{dx_1} = -h_1(T_0^{p+1} - T_{air}^{p+1}) + a_{glass} G_T^{p+1} \rightarrow$$

$$-\left(\frac{k_1}{dx_1}\right) T_1^{p+1} + \frac{k_1}{dx_1} T_0^{p+1} + h_1 T_0^{p+1} = h_1 T_{air}^{p+1} + a_{glass} G_T^{p+1} \rightarrow$$

$$\left(\frac{k_1}{dx_1} + h_1\right) T_0^{p+1} - \left(\frac{k_1}{dx_1}\right) T_1^{p+1} = h_1 T_{air}^{p+1} + a_{glass} G_T^{p+1} \quad (12)$$

Lower surface (i=n-1)

Lower surface suffers heat losses due to radiation Q_{rad} and convection Q_{conv}.

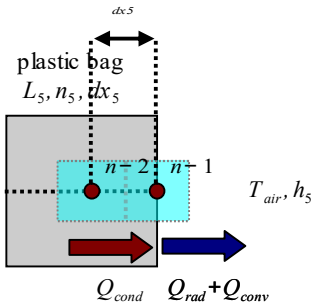

Figure 7 Lower surface boundary condition (i=n-1)

Following a similar approach, we assume a heat transfer coefficient h_5, such as:

$$h_5 = h_{c5} + h_{r5} \quad (13)$$

$$-k_5 \frac{T_{n-1}^{p+1} - T_{n-2}^{p+1}}{dx_5} = h_5(T_{n-1}^{p+1} - T_{air}^{p+1}) \rightarrow$$

$$-\left(\frac{k_5}{dx_5}\right) T_{n-1}^{p+1} + \frac{k_5}{dx_5} T_{n-2}^{p+1} - h_5 T_{n-1}^{p+1} = -h_5 T_{air}^{p+1} \rightarrow$$

$$-\left(\frac{k_5}{dx_5}\right) T_{n-2}^{p+1} + \left(\frac{k_5}{dx_5} + h_5\right) T_{n-1}^{p+1} = h_5 T_{air}^{p+1} \quad (14)$$

The calculation of the combined convection-radiation coefficients h_1, h_5 is a complex procedure (either mathematical or experimental) and is beyond the scope of this present simplified approach [19]. For the purposes of the present thesis and the sake of simplicity, a relatively low value was chosen which was constant and equal for both surfaces. As it has been previously mentioned, in some cases a PV module cell can operate by 30 ºC higher than the ambient temperature. In order to achieve a 30 ºC temperature difference during the month of July, which in terms of Athens is the warmest period, a parametric study, with h_1, h_5 as parameters, yielded:

$$h_1 = h_5 = 4\left[\frac{W}{m^2 K}\right] \quad (15)$$

Initial conditions

We assume initial temperature of every node equal to the ambient temperature:

$$T_i^0 = T_{air}^0 \text{ , i=0,1,2,….,n-1} \quad (16)$$

System of equations

The above result to the following system of linear equations:

$$\left(\frac{k_1}{dx_1}+h_1\right)T_0^{p+1}-\left(\frac{k_1}{dx_1}\right)T_1^{p+1}=h_1T_{air}^{p+1}+a_{glass}G_T^{p+1} \quad \text{i=0}$$

$$(-r_i dx_i)T_{i-1}^{p+1}+(1+r_i(dx_{i-1}+dx_i))T_i^{p+1}-(r_i dx_{i-1})T_{i+1}^{p+1}=T_i^p \quad \text{i=1÷n-2}$$

$$-\left(\frac{k_5}{dx_5}\right)T_{n-2}^{p+1}+\left(\frac{k_5}{dx_5}+h_5\right)T_{n-1}^{p+1}=h_5T_{air}^{p+1} \quad \text{i=n-1}$$

The air temperature T_{air} was taken from the historic data of the National Technical University of Athens' meteorological station [20]. G_T was calculated based on empirical equations specific to the city of Athens and for a surface angle of $\beta=\varphi=37.97^o$ (maximum insolation over the course of one year) [17].

Systems of linear equations are usually solved with the Gaussian elimination method. In our case, the above system has a tridiagonal form (coefficient matrix is mostly vacant apart from three main diagonals) and for that, TDMA (TriDiagonal Matrix Algorithm) was used. TDMA or Thomas algorithm is an adaptation of the Gaussian elimination method that is used specifically for tridiagonal matrices in order to reduce computational time [6-8].

EFFECTIVE HEAT CAPACITY

One of the most popular methods for modeling phase change materials is the effective heat capacity method. It is distinguished for its ease of use since it replaces the PCM's heat capacity, $C_{p,pcm}$, with an effective heat capacity, $C_{p,eff}=C_{p,eff}(T)$, a function of temperature, in the heat equation which describes the problem. In other words:

$C_p = C_{p,s}$, $T < T_s$, solid phase

$C_p = C_{p,eff}$, $T_s \le T \le T_l$, phase change

$C_p = C_{p,l}$, $T > T_l$, liquid phase

The use of this method demands the complete expression for the effective heat capacity of a phase change material as a function of temperature. This paper was based on the published research that took place for specific phase change materials, mainly paraffins (greek paraffin, RT20, RT27, RT58) and a high density non-flammable inorganic PCM (SP25A8) [10]. Among those materials possible candidates are those whose phase change occurs close to 25 ºC, the ideal cell operating temperature. Those materials are RT20 (15-26 ºC, H=132.1 kJ/kg), RT27 (22-31 ºC, H=167.4 kJ/kg) and SP25A8 (22-32 ºC, H=141.5 kJ/kg). Full expressions of their effective heat capacity, a comparative plot and a properties table follow. It should be noted that paraffins due their relatively high latent heat capacities, their compatibility with other materials (e.g. containers), their chemical stability and the fact that they are non-corrosive and non-toxic makes them excellent candidates for matters of thermal control [21].

RT20

$$C_{p,eff}(T)=444.4711352-170.5210626T+25.80658991T^2$$
$$-1.912462169T^3+0.06910480624T^4-0.0009667426392T^5$$
$$\text{for } 15^oC \le T \le 19.5^oC \quad (17)$$

$$C_{p,eff}(T)=5529.086311-565.4394794T+14.50378915T^2$$
$$\text{for } 19.5^oC < T \le 20.5^oC \quad (18)$$

$$C_{p,eff}(T)=3780.001949-342.8478233T+7.797040983T^2$$
$$\text{for } 20.5^oC < T \le 22^oC \quad (19)$$

$$C_{p,eff}(T)=3735.906512-536.9879458T+28.98735267T^2$$
$$-0.6959772441T^3+0.006270432248T^4$$
$$\text{for } 22^oC < T \le 26^oC \quad (20)$$

RT27

$$C_{p,eff}(T)=-329.5000062+106.3162953T-13.35423683T^2$$
$$+0.8223480772T^3-0.02488671396T^4+0.0002972388922T^5$$
$$\text{for } 22^oC \le T \le 25^oC \quad (21)$$

$$C_{p,eff}(T)=9542.790195-774.7503271T+15.74031481T^2$$
$$\text{for } 25^oC < T \le 26.8^oC \quad (22)$$

$$C_{p,eff}(T)=41611.7679-3023.692869T+54.96396748T^2$$
$$\text{for } 26.8^oC < T \le 27.5^oC \quad (23)$$

$$C_{p,eff}(T)=31155.44075-3820.483549T+175.7678837T^2$$
$$-3.594806096T^3+0.02757236338T^4$$
$$\text{for } 27.5^oC < T \le 31^oC \quad (24)$$

SP25A8

$$C_{p,eff}(T)=-5822.7083+1559.960873T-166.178906T^2$$
$$+8.806172538T^3-0.2322802438T^4+0.002441877714T^5$$
$$\text{for } 22^oC \le T \le 23.8^oC \quad (25)$$

$$C_{p,eff}(T)=30643.84674-2584.495777T+54.51400097T^2$$
$$\text{for } 23.8^oC < T \le 24.5^oC \quad (26)$$

$$C_{p,eff}(T)=2456.776607-177.5933256T+3.228251256T^2$$
$$\text{for } 24.5^oC < T \le 27.2^oC \quad (27)$$

$$C_{p,eff}(T)=-3900.417315+553.0906948T-28.64445051T^2$$
$$+0.6468310842T^3-0.005396817351T^4$$
$$\text{for } 27.2^oC < T \le 32^oC \quad (28)$$

Table 2 Properties of the materials RT20, RT27 and SP25A8

Property	RT20	RT27	SP25A8
ρ [kg/m^3]	880	880	1500
k [W/mk]	0.2	0.2	0.6
C_p [kJ/kgK]	$C_{p,eff}(T)$	$C_{p,eff}(T)$	$C_{p,eff}(T)$
C_{ps} [kJ/kgK]	1.9	2.0	2.6
C_{pl} [kJ/kgK]	2.5	2.3	2.7
T_s [ºC]	15	22	22
T_l [ºC]	26	31	32
H [kJ/kg]	132.1	167.4	141.5

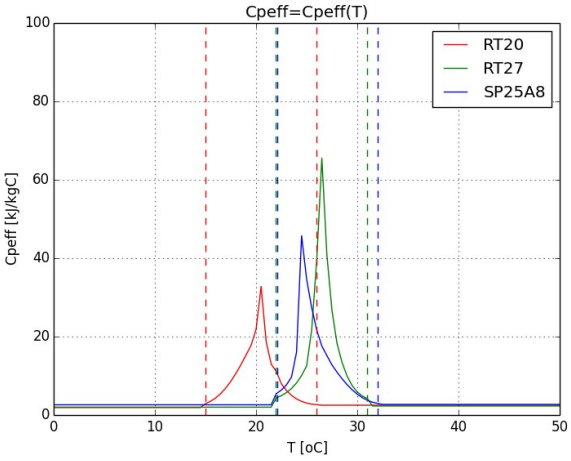

Figure 8 Comparative plot of $C_{p,eff}$ for the three PCMs

RESULTS

The purpose of this paper was to develop a simplified algorithm that calculates a photovoltaic module's cell temperature both as a unit and as a system in direct contact with a phase change material. That way the possibility of using phase change materials as a mean of thermal control can be assessed. PCM's were modeled based on the effective heat capacity method and a relative published research on specific materials.

So far, a series of assumptions have been made:

- Simplified PV panel geometry.
- Perfect contact between PV-PCM.
- One-dimensional heat transfer.
- Constant heat conductivity for every material.
- A combined heat transfer coefficient that takes free convection and radiation into account.
- Insolation was calculated based on empirical equations and a surface angle that corresponds to maximum annual energy.
- Air temperature was based on real data retrieved from the National Technical University of Athens' meteorological station.

The three first days of each month between each month from January till August were considered as periods of interest. After the summer, both air temperature and solar radiation begin to drop so it was deemed unnecessary to study further periods of time [17]. For conciseness, only the results of three most representative periods will be presented (January, April and July).

The first three figures at each period (figures 9, 10, 11, 13, 14, 15, 17, 18 and 19) give a general depiction of the temperature levels inside each PCM. They also give a measure of the efficiency of each material. In an ideal scenario a PCM would fully enter and exit the two-phase region (area between the two dashed lines) during the course of each day. Unfortunately, under real conditions that rarely occurs, since most PCMs are effective in a very small temperature region.

The last figure at each period (figures 12, 16 and 20) gives the cell temperature over time in each case. At a first look different materials are more efficient at different periods. A PCM's efficiency at reducing cell temperature is also reflected at the internal PCM temperature.

During the first period (1-3/1) figures 9, 10, 11 show that RT20 enters almost completely the two-phase region while RT27 and SP25A8 enter it partially. This is also reflected in figure 12, where RT20 produces lower temperatures. During the second period (1-3/4) and according to figure 16, even though the PV-RT20 system starts with lower temperatures, RT27 is more efficient, providing a better thermal control and ending up with lower temperatures. This is evident in figures 13, 14, 15 where RT27 enters the two-phase region while RT20 and SP25A8 enter the liquid phase. It should be noted that despite that fact that RT27 and SP25A8 display similar thermo-physical properties, SP25A8 consistently under-performs compared with RT27. This is attributed to the SP25A8's higher density. During the summer period (1-3/7) a gradual increase in the cell temperature levels is noticeable in all cases. In fact, cell temperature ends up higher than in the case of a PV panel without the use of PCM (figure 20). This is anticipated since all PCMs enter the liquid phase during the day without being able to release the absorbed heat during the night. This is attributed to the very low heat conductivity (RT20 and RT27: 0.2 W/mK, SP25A8: 0.6 W/mK) that makes them function as heat insulators above a certain temperature level.

Overall, with the exclusion of the summer period when all materials end up performing poorly, RT27 achieves better results. Even during the winter period where it under-performs compared with RT20 it still yields a considerable temperature reduction.

CONLUSIONS

The present thesis has produced a series of conclusions:

- All phase change materials are extremely effective in specific temperature regions.
- Comparing the three phase change materials it can be said that RT27 proves to be more suitable along the course of a year.
- Above a certain temperature level all three PCMs act as thermal insulators. The fact that they have low relative thermal conductivities inhibits the rate with which they expel the absorbed heat during the night.

- Two methods to increase the efficiency of the PCM candidates are forced convection (i.e. fans) and the insertion of a metal meshes [3,21].

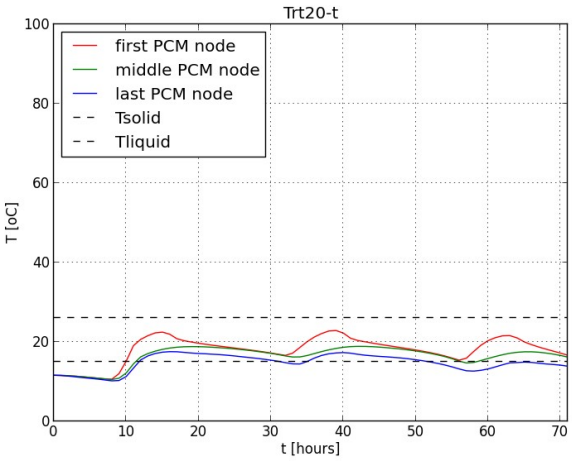

Figure 9 Temperature distribution inside RT20, 1-3/1

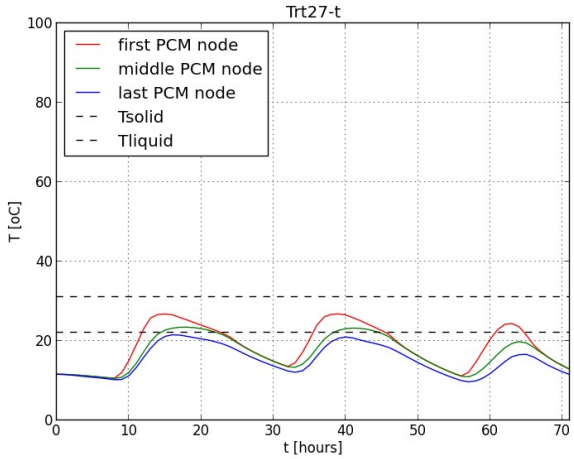

Figure 10 Temperature distribution inside RT27, 1-3/1

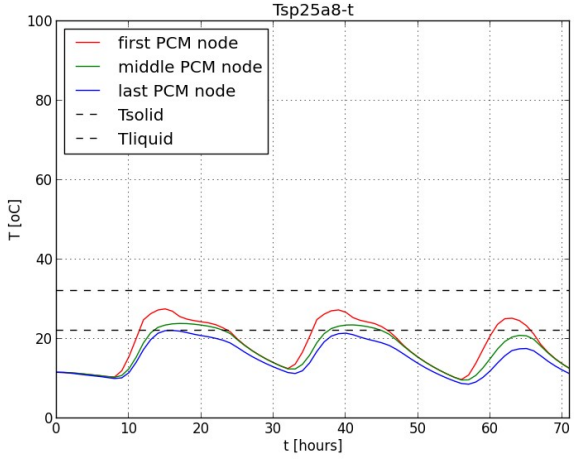

Figure 11 Temperature distribution inside SP25A8, 1-3/1

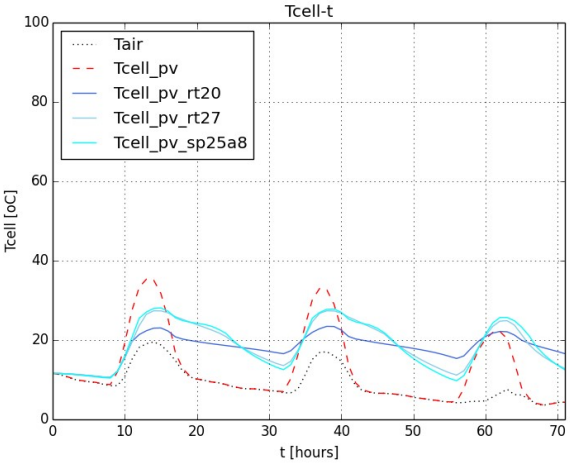

Figure 12 Cell temperature comparative plot, 1-3/1

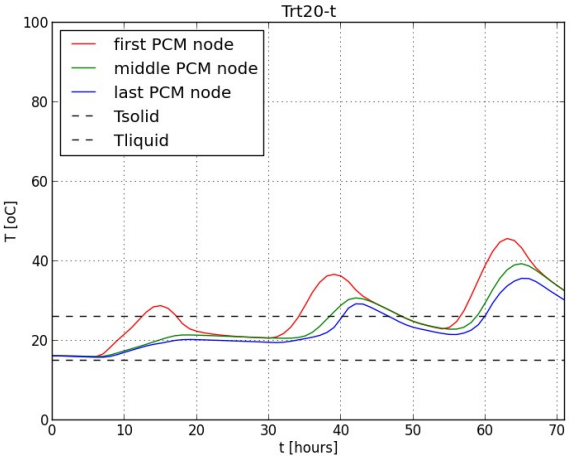

Figure 13 Temperature distribution inside RT20, 1-3/4

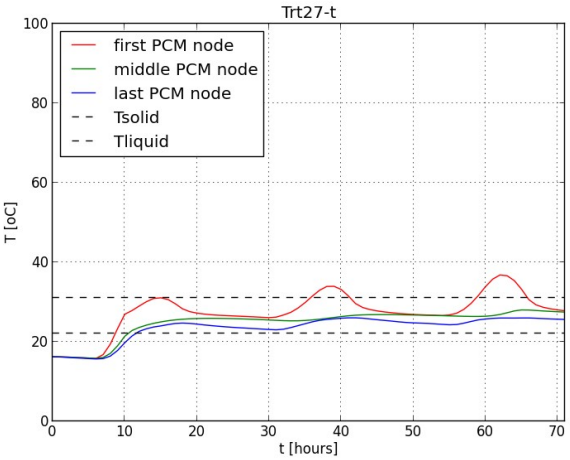

Figure 14 Temperature distribution inside RT27, 1-3/4

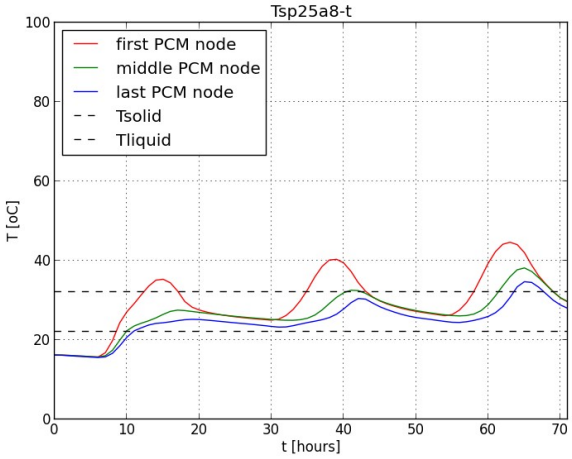

Figure 15 Temperature distribution inside SP25A8, 1-3/4

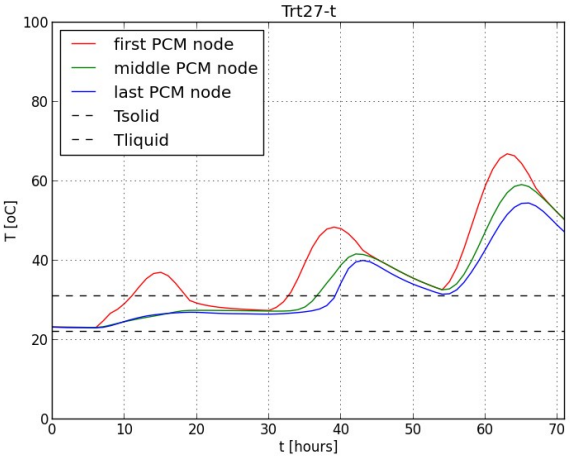

Figure 18 Temperature distribution inside RT27, 1-3/7

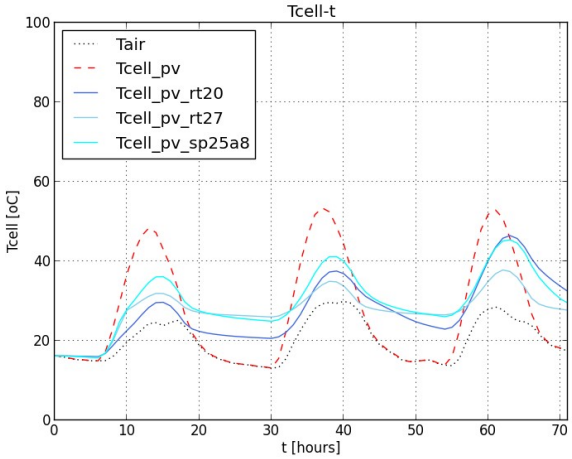

Figure 16 Cell temperature comparative plot, 1-3/4

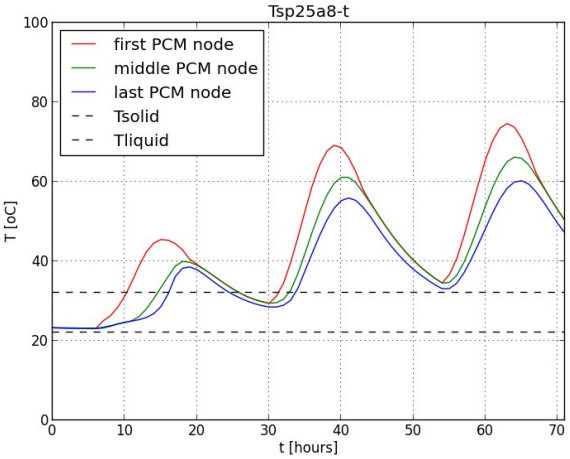

Figure 19 Temperature distribution inside SP25A8, 1-3/7

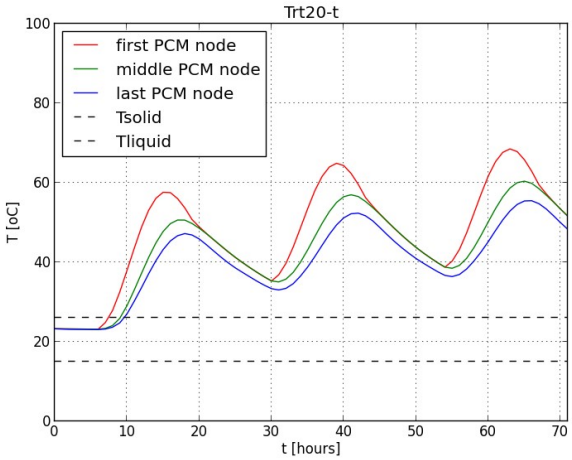

Figure 17 Temperature distribution inside RT20, 1-3/7

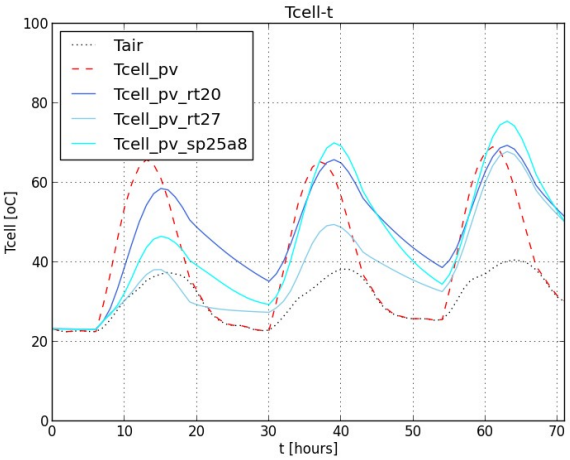

Figure 20 Cell temperature comparative plot, 1-3/7

REFERENCES

[1]. A. Luque, S. Hegedus. "Handbook of photovoltaic and science and engineering". New Jersey: John Wiley & Sons. 2011. 2nd edition.

[2]. R. H. Plante. "Solar energy, photovoltaics and domestic hot water". Oxford: Elsevier science press. 2014. 1st edition.

[3]. D. V. Hale, M. J. Hoover, M. J. O'Neill. "Phase change materials handbook". Alabama: NASA report. 1971.

[4]. "Wikipedia:Phase change material". 2012. Retrieved from: https://en.wikipedia.org/wiki/Phase-change_material

[5]. N. Papamanolis. "Econ3: Building applications of phase change materials". 2015. Retrieved from: http://www.econ3.gr/readmore.php?article_id=51771295788153

[6]. G. Mpergeles. "Computational fluid dynamics". Athens: Simeon Publishing. 2006. 4th edition.

[7]. K. X. Giannakoglou, I. Anagnostopoulos, G. Mpergeles. "Numerical analysis for engineers". Athens: National Technical University of Athens Publishing. School of Mechanical Engineering. 2003. 3rd edition.

[8]. J. Kiusalaas. "Numerical methods in engineering with Python 3". New York: Cambridge University Press. 2013. 1st edition.

[9]. K. Aspromallis, K. A. Antonopoulos. "Prediction of phase change materials (PCM) efficiency in greek buildings by use of the Finite Difference Method". Master's thesis. National Technical University of Athens, School of Mechanical Engineering. 2014.

[10]. E. D. Kravaritis, K. A. Antonopoulos, C. Tzivanidis. "Experimental determination of the effective heat capacity function and other properties for various phase change materials using the thermal delay model". Applied Energy 88(2011)4459-4469.

[11]. "Kyocera: KC175GHT specifications". Retrieved from: http://www.kyocerasolar.com/assets/001/5191.pdf

[12]. L. L. Kazmerski. "Photovoltaics: A review of cell and module technologies". Renewable and sustainable energy review. Vol. 1, Nos ½, pp. 71-170, 1997.

[13]. "MakeItFrom: Material properties database". Retrieved from: http://www.makeitfrom.com

[14]. F. P. Incropera, D. P. DeWitt, T. L. Bergman. "Fundamentals of heat and mass transfer". New Jersey: John Wiley & Sons. 2006. 6th edition.

[15]. A. Steggou, Z. Sagia. "Heat transfer". Athens: National Technical University of Athens, School of Mechanical Engineering. 2015. 1st edition.

[16] K. X. Kakatsios. "Heat transfer". Athens: Kleidarithmos Publishing. 2002. 1st edition.

[17]. K. A. Antonopoulos. "Thermal-solar systems". Athens: National Technical University of Athens Publishing, School of Mechanical Engineering. 2004. 1st edition.

[18]. E. Marin. "Linear relationships in heat transfer". Lat. Am. J. Phys. Educ. Vol. 3, No. 2, May 2009:243-245

[19]. M. Sakin, F. Kaymak-Ertekin, C. Ilicali. "Convection and radiation combined surface heat transfer coefficient in baking ovens". Journal of Food Engineering 94 (2009) 344-349.

[20]. "National Technical University of Athens' meteorological station. Department of Water Resources and Environmental Engineering". Retrieved from: http://openmeteo.org/stations/d/1334/

[21]. N. Sahan, M. Fois, H. Paksoy. "Improving thermal conductivity phase change materials-A study of paraffin nanomagnetite composites". Solar Energy Materials & Solar Cells 137 (2015) 61-67.